Separation Science and Technology
Publication details, including instructions for authors and subscription information:
http://www.informaworld.com/smpp/title~content=t713708471

Gradient Hydroxyapatite Chromatography with Small Sample Loads. II. Experimental Analysis and the Resolving Power of the Columns

Tsutomu Kawasaki[a]
[a] LABORATOIRE DE GENETIQUE MOLECULAIRE INSTITUT DE RECHERCHE EN BIOLOGIE MOLECULAIRE FACULTE DES SCIENCES, PARIS, FRANCE

To cite this Article Kawasaki, Tsutomu(1981) 'Gradient Hydroxyapatite Chromatography with Small Sample Loads. II. Experimental Analysis and the Resolving Power of the Columns', Separation Science and Technology, 16: 5, 439 — 473
To link to this Article: DOI: 10.1080/01496398108068532
URL: http://dx.doi.org/10.1080/01496398108068532

SEPARATION SCIENCE AND TECHNOLOGY, 16(5), pp. 439–473, 1981

Gradient Hydroxyapatite Chromatography with Small Sample Loads. II. Experimental Analysis and the Resolving Power of the Columns

TSUTOMU KAWASAKI

LABORATOIRE DE GENETIQUE MOLECULAIRE
INSTITUT DE RECHERCHE EN BIOLOGIE MOLECULAIRE
FACULTE DES SCIENCES
PARIS 5, FRANCE

Abstract

Several chromatograms of biological macromolecules on hydroxyapatite columns were analyzed on the basis of a theory previously developed. The experimental data confirm the validity of the theory. The optimal chromatographic conditions were explored by introducing experimental data into the theory. In many instances it is indispensable that the slope of the molarity gradient of competing ions used in elution be extremely small to obtain high resolution; this slope generally is much too steep in published chromatograms. The differences in adsorption energies per molecule between the collagen components present in the neighboring peaks of the multipeak chromatogram obtained in an earlier paper were measured. These gave a value of about 0.5 kcal/mol for any pair of peaks. This should correspond to the energy of adsorption for a functional carboxyl group onto a C site. The same value was obtained in an earlier paper by an independent method on the basis of a microheterogeneous model of collagen. The agreement strongly supports the microheterogeneous model.

INTRODUCTION

On the basis of experimental data, a model has been derived for the adsorption and desorption phenomena of sample molecules on the crystal surfaces of hydroxyapatite (HA) in a column. This model can be stated briefly as follows: adsorbing sites are arranged in some manner (see below) on the surface of HA, and sample molecules with functional or adsorption groups compete with particular ions from the buffer for these adsorbing sites (*1*). Both the distribution and stereochemical structures of adsorbing

sites on the surface of HA were explored on the basis of crystallographic data with the aid of chromatographic data. Thus two types of sites, referred to as P and C sites, exist on different crystal surfaces of HA. Of the molecules that are investigated in the present paper, lysozyme, cytochrome c, and poly-L-lysine are adsorbed onto P sites by using functional basic groups [ε-amino groups in the case of poly-L-lysine (with a long enough polypeptide chain)], and these molecules compete with potassium or sodium ions from the buffer for P sites. Collagen and nucleoside polyphosphates are adsorbed onto C sites by using carboxyl and phosphate groups, respectively, and these compete with phosphate ions from the buffer for C sites. Concerning T_2 phage particles, we have no experimental data to show onto which crystal sites they are adsorbed. (For details, see the section entitled "Analysis of Several Experiments" and Ref. *1*.)

When dealing with small sample loads on HA columns, the chromatographic behavior of any single component in the mixture is independent of the other components (*1*). This has been verified experimentally (*2*). In Ref. *1* a new theory of HA chromatography was developed, and equations representing theoretical chromatograms with small sample loads were derived for both gradient and stepwise chromatographies. These equations are summarized in Appendix I, including brief explanations for the physical meanings of any symbols that appear in the equations. It should be emphasized that the chromatographic mechanisms are fundamentally different between gradient and stepwise chromatographies. No theories that have been developed over many years for stepwise chromatography are applicable to gradient chromatography (*1*). In the present paper, experimental results obtained for several different molecules (see above), mainly for the case of gradient chromatography, are analyzed on the basis of the equations obtained in Ref. *1*. The validity of the theory developed in Ref. *1* is confirmed experimentally. The resolving power of the column is investigated, and the optimal chromatographic conditions are explored.

ANALYSIS OF SEVERAL EXPERIMENTS

Lysozyme; Some Predictions Obtained from the Analysis *

Lysozyme is a basic enzymatic protein with molecular weight 1.43×10^4 daltons and an approximate prolate spheroid shape of dimensions $45 \times 30 \times 30$ Å (*3*). Lysozyme is adsorbed onto P crystal sites through basic functional groups, and the elution of the molecule is carried out by competition with potassium ions from the buffer for P sites (*4*).

*This will be verified by other experiments in the following two subsections.

By using this molecule, important data for gradient chromatography with small sample loads were obtained. Thus a number of experiments were carried out by changing both the length, L, of the column and the slope, g, of the molarity gradient over wide ranges of these parameters (*2*). It was shown (*2*) that both the elution molarity at the center of gravity of the chromatographic peak and the standard deviation of the peak depend upon both L and g. The results of these experiments are shown in both Fig. A1 in Appendix II and Fig. 1 (for explanations of the figures, see below). Therefore, let us begin with examining whether or not these data can quantitatively be explained by our theory.

Figure A1 in Appendix II illustrates experimental plots of elution molarities at centers of gravity of lysozyme chromatographic peaks versus L of the column for three different slopes of the molarity gradient. Elution molarity is expressed as molarity of the phosphate ions in the buffer; this is 2/3 the molarity of competing potassium ions (see Table 2). The three slopes, g, of the gradient expressed as those concerning potassium ions (written hereafter as $g_{(K^+)}$) are 1.18×10^{-3}, 4.24×10^{-4}, and 3.53×10^{-5} M/cm. It can be seen in Fig. A1 that the dependence of elution molarity upon column length differs when the slope of the molarity gradient applied is different, giving three curves corresponding to the three values of $g_{(K^+)}$.

The elution molarity at the center of gravity of a theoretical peak essentially is equal to the elution molarity for a hypothetical sharp peak occurring provided there is no longitudinal molecular diffusion in the column (Appendix I; cf. Figs. 5 and 11). Equation (A14) shows that elution molarity, m, of the hypothetical sharp peak can be represented as a function of a parameter s defined as the product of g and L (Eq. A3). Therefore, if our theory is correct, the three curves in Fig. A1 should converge into a single curve when elution molarity is plotted versus s instead of L. The points in Fig. A2 in Appendix II are experimental plots of ln s versus elution molarity of the experimental points in Fig. A1, where s and the elution molarity are written as $s_{(K^+)}$ and $m_{elu(K^+)}$, respectively, indicating that these now concern potassium ions in the buffer. Figure A2 demonstrates that the three curves in Fig. A1, in fact, converge into a single arrangement, confirming the correctness of the theory.

Continuous curves in Fig. A2 are theoretical ones calculated by using Eq. (A14). A best fit with the experiment can be obtained by assuming $\varphi' = 9\ M^{-1}$ (the parameter characteristic of competing ions; cf. Eqs. A4 and A5), and $x' = 7$ and $\ln q = 6.7$ (the parameters characteristic of lysozyme; cf. Eqs. A4–A6). (For details, see Ref. *5*. In Ref. *5*, φ' was represented as a dimensionless quantity. φ' should have a dimension of M^{-1}, however.) It should be noted that the coincidence of the theoretical curve with the experimental plot is good, explaining a slight displacement

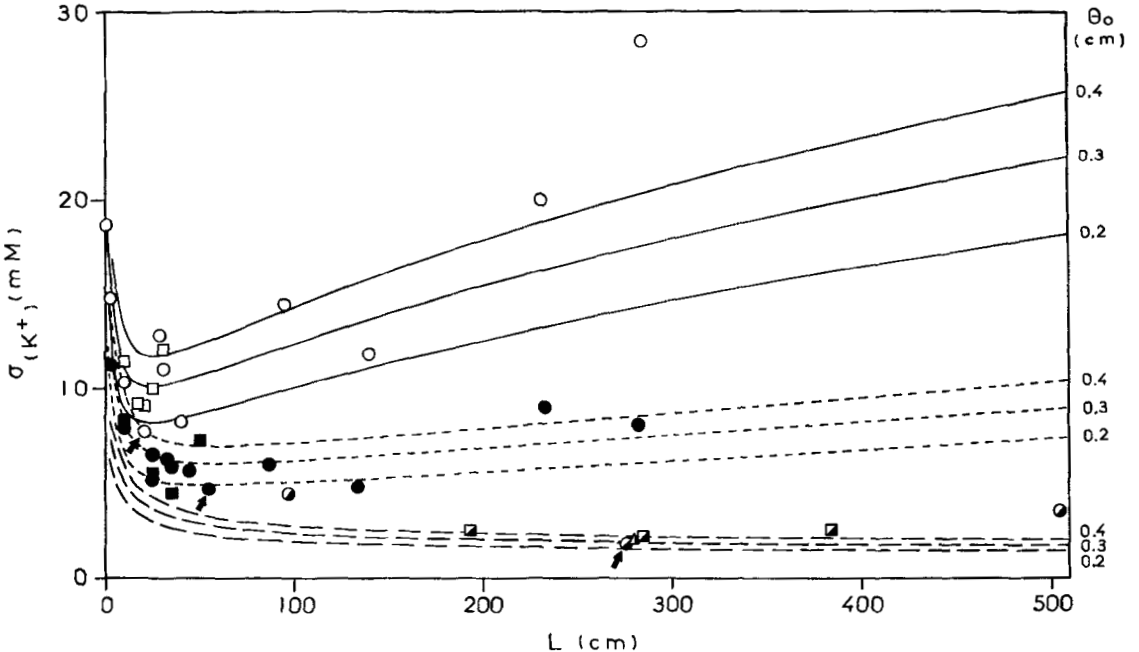

FIG. 1. The points are experimental plots of $\sigma_{(K^+)}$ of the chromatographic peaks of lysozyme vs length, L, of the column for three different slopes of the gradient of potassium ions, $g_{(K^+)} = 1.18 \times 10^{-3}$ (○, □), 4.24×10^{-4} (●, ■), and 3.53×10^{-5} (◭, ◕, ◪) (M/cm). (Reproduced, with modifications, from Fig. 6 of Ref. *2*). All the experimental points correspond to the points in both Figs. A1 and A2, the three points indicated by arrows corresponding to the three points also indicated by arrows in these figures. The experimental chromatograms for these three points are illustrated in Figs. 6(a), (b), and (c). The curves are theoretical, calculated for the three values of $g_{(K^+)}$: 1.18×10^{-3} (——), 4.24×10^{-4} (- -), and 3.53×10^{-5} (– –) (M/cm), and for three values of θ_0. It can be seen that a best fit with the experiment is achieved when $\theta_0 = 0.3$ (cm).

from the linearity of the arrangement of the experimental points (see Fig. A2). Further, the values of both x' and $\ln q$ assumed above are reasonable from a stereochemical point of view (*5*). The value of φ' given above coincides satisfactorily with the value deduced from the independent experiment of poly-L-lysine (*5*). These again confirm the theory. All calculations below will be carried out on the basis of the experimental values of the parameters obtained above.

The points in Fig. 1 are experimental plots of the standard deviation, $\sigma_{(K^+)}$, of the chromatographic peaks that correspond to the experimental points in both Figs. A1 and A2 versus L. The standard deviation is expressed as the range of potassium molarities (mM) in which the peak appears. The theoretical curves in Fig. 1 were calculated by using Eqs. (A1) and (A2) (and A3–A6) for the three values of $g_{(K^+)}$ and for three values of the parameter θ_0. θ_0 represents the longitudinal diffusion of molecules in the column (see Eq. A1). It can be seen in Fig. 1 that the variations in the positions of the experimental points around the theoretical curves are larger than the variation seen in Fig. A2. The experiments with extremely long columns were carried out by connecting several short columns with capillary tubes (*2*). It is presumed that considerable deviation of the experimental results from the theoretical predictions occurr, for instances, at $L \approx 280$ cm when $g_{(K^+)} = 1.18 \times 10^{-3}$ M/cm, and at $L \approx 500$ cm when $g_{(K^+)} = 3.53 \times 10^{-5}$ M/cm in Fig. 1, due to abnormal molecular diffusions occurring at the joints of the columns. The mean positions of the chromatographic peaks, nevertheless, are hardly influenced by these diffusions (Figs. A1 and A2). It can be seen in Fig. 1, however, that the following fundamental aspects are satisfactorily explained by the theory: (a) $\sigma_{(K^+)}$, in general, decreases rapidly with an increase of L when L is small, but that $\sigma_{(K^+)}$ increases slowly after the first rapid decrease [with $g_{(K^+)} = 3.53 \times 10^{-5}$ M/cm, the theoretical increase of $\sigma_{(K^+)}$ with an increase of L should occur when L is larger than 500 cm]; and (b) from the ratios among $\sigma_{(K^+)}$ for the three different values of $g_{(K^+)}$ occurring at any value of L (except some cases; see above), relevant to the satisfactory coincidence for these ratios between the theory and the experiment, a best value, 0.3 cm, of the parameter θ_0 can be obtained (see Fig. 1). This coincidence is important because the theoretical prediction stating that the resolution of the column, in general, should increase with a decrease in the slope of the molarity gradient (see below) mainly depends upon how the standard deviation, σ, of a chromatographic peak (expressed in units of molarity; see above) decreases with a decrease in g of the gradient. This prediction is quite general and holds almost independently of the value of θ_0 (except for the prediction concerning the exact value of R_s that should be obtained under a given experimental condition; see below).

Since Eqs. (A1) and (A2) (and Eq. A14) are now experimentally confirmed, it is possible to predict the resolving power of the column for several types of molecular mixtures under different experimental conditions. We limit ourselves, however, to the case when L is less than 300 cm. (Practically, it is not easy to perform the experiment with a column longer than 300 cm.) We express the resolving power of the column in terms of the parameter R_s:

$$R_s = \Delta z/4\bar{\sigma} \tag{1}$$

where Δz is the distance between the centers of the two chromatographic peaks under consideration and $\bar{\sigma}$ is the average standard deviation of these peaks, the factor 4 being inserted for convenience. Equation (1) has already been used by some authors (*6*).

Let us consider, for instance, a chromatographic separation of lysozyme from a hypothetical molecule with the same molecular dimensions. Thus it will have the same value, 7, of x' as that for lysozyme, but the value of $\ln q$ (see Eq. A6) will be larger by a factor of $\ln 2 = 0.7$ than the 6.7 value for lysozyme, i.e., with the value 7.4 for $\ln q$. If the hypothetical molecule is adsorbed onto the HA surface by using the same (average) number, x, of basic groups as for lysozyme, but if the total number and/or the distribution of these groups on the molecular surface are (is) different, the value of $\ln \tau$ or $\ln q$ can be larger by a factor $\ln 2$ than that for lysozyme (see Eq. A6). If the molecule is adsorbed with an excess of the basic group compared with lysozyme, the value of $\ln q$ should be still larger because it can be estimated (*5*) that the value of ε for a basic group should be 2–2.2 kcal/mol. The value of ε/kT should be 3.4–3.7 at 25°C (Eq. A6). The curves indicated by $x' = 7$ in Fig. 2 illustrate the theoretical dependences, calculated by using Eqs. (A1) and (A2) and the value 0.3 cm for θ_0, of $\sigma_{(K^+)}$ upon L for lysozyme (the lower curves of the pairs indicated by $x' = 7$). The hypothetical molecule above is shown in the upper curves of the pairs for three different $g_{(K^+)}$ which are identical with the three $g_{(K^+)}$ in Fig. 1. The curves corresponding to the same $g_{(K^+)}$ are drawn with common symbols in Figs. 1 and 2. The lower curves of the pairs indicated by $x' = 7$) in Fig. 2, therefore, are identical with the curves for $\theta_0 = 0.3$ cm in Fig. 1. It can be seen in Fig. 2 that $\sigma_{(K^+)}$ should depend only slightly upon $\ln q$.

The curves indicated by $x' = 7$ in Fig. 3 are plots of $\sigma_{(K^+)}$ as a function of $g_{(K^+)}$ for three different column lengths (10, 50, and 300 cm) for lysozyme (continuous curves) and hypothetical molecule (dotted curves). The three vertical lines in Fig. 3 indicate the three $g_{(K^+)}$ in Figs. 1 and 2.

By using Eqs. (A1) and (A2) it also is possible to calculate the dependences of the elution potassium molarities, $m_{elu(K^+)}$, of the center of gravity

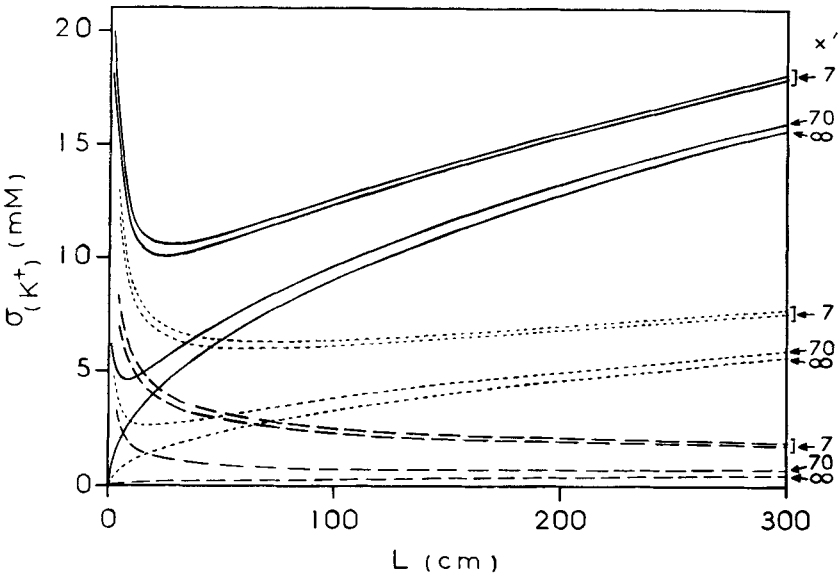

FIG. 2. Theoretical dependence of $\sigma_{(K^+)}$ upon L for the three different values of $g_{(K^+)}$ in Fig. 1 (shown by the same symbols as in Fig. 1) for molecules (adsorbed onto P sites) with different values, 7, 70, and ∞ of x', obtained by using the value 0.3 cm of θ_0. The curves for $x' = \infty$ (which are parabolas) were calculated by using Eq. (A11'). The lower and the upper curves of the pairs indicated by $x' = 7$ represent the curves for lysozyme and those for a hypothetical molecule with the same dimensions as those of lysozyme but with a slightly larger value of ln q, respectively, the former being identical with the curves indicated by $\theta_0 = 0.3$ cm in Fig. 1. (For details, see text.)

of the chromatographic peaks upon both L and $g_{(K^+)}$. It can be shown that these curves are almost identical with the curves for the elution molarities of the sharp chromatographic peaks, calculated from Eq. (A14), assuming that there is no longitudinal molecular diffusion in the column (see above; cf. Fig. 5). The curve for lysozyme calculated from Eq. (A14) and plotted on another plane is shown in Fig. A2 in Appendix II. Now, the dependences of the difference, $\Delta m_{elu(K^+)}$, in elution potassium molarities between lysozyme and the hypothetical molecule upon both L and $g_{(K^+)}$ can be obtained. $\Delta m_{elu(K^+)}$ depends only slightly upon both L and $g_{(K^+)}$ except for very small values of L and $g_{(K^+)}$; $\Delta m_{elu(K^+)}$ converges rapidly to zero as one of these tends to zero.

By substituting the average value of $\sigma_{(K^+)}$ and the value of $\Delta m_{elu(K^+)}$ obtained under different experimental conditions into the terms $\bar{\sigma}$ and Δz in Eq. (1), respectively, the resolution R_s of the column for the mixture of lysozyme and the hypothetical molecule under different experimental

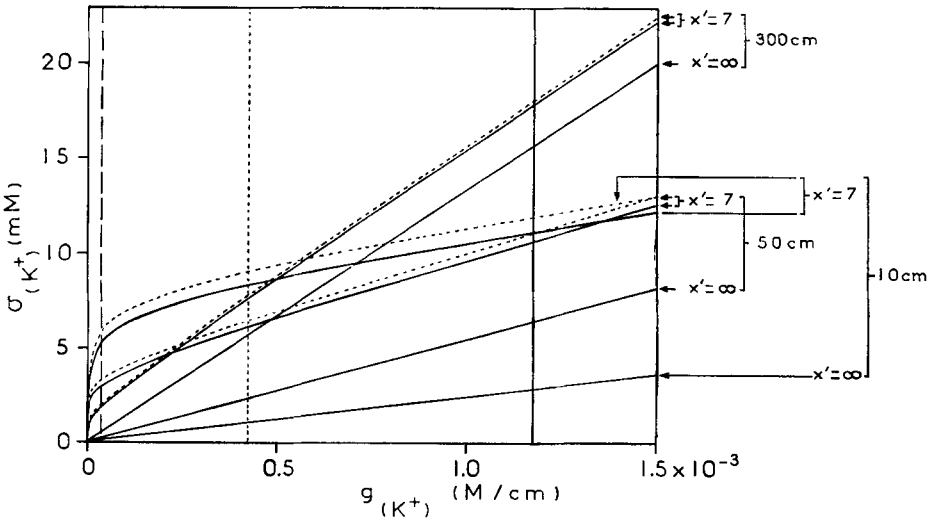

FIG. 3. Theoretical dependences of $\sigma_{(K^+)}$ upon $g_{(K^+)}$ for three different values, 10, 50, and 300 cm, of L for molecules adsorbed onto P sites with the values 7 and ∞ of x' obtained by using the value 0.3 cm of θ_0. The curves for $x' = \infty$ (which are straight lines) were calculated by using Eq. (A11'). The lower continuous and the upper dotted curves of the pairs indicated by $x' = 7$ represent the curves for lysozyme and those for the hypothetical molecule with the same dimensions as those of lysozyme but with a slightly larger value of $\ln q$ (considered in Fig. 2), respectively. The three vertical lines indicate the three $g_{(K^+)}$s in both Figs. 1 and 2. (For details, see text.)

conditions can be calculated. The result of such calculations is shown in Fig. 4. Thus the three curves in Fig. 4 represent R_s as functions of $g_{(K^+)}$ for three different L: 10, 50, and 300 cm. In Fig. 4 are also shown the three $g_{(K^+)}$ in Figs. 1 and 2 (three vertical lines) and the resolutions of the column under conditions in three experiments indicated by arrows in Fig. 1 (three points). It can be seen in Fig. 4 that R_s increases, in general, with a decrease of $g_{(K^+)}$. When $g_{(K^+)}$ is large, R_s depends only slightly on L but increases slightly with a decrease of L.* On the other hand, when $g_{(K^+)}$ is small, R_s increases considerably with an increase of L, and the maximum resolution can be achieved by using a minimum slope of the molarity gradient and a maximum length of the column. The maximum value of R_s (about 3.9, estimated by extrapolation) can be obtained for a mixture of lysozyme and the hypothetical molecule by using the limiting value $+0$ M/cm for $g_{(K^+)}$

*In Fig. 4, at the maximum value of $g_{(K^+)}$ or when $g_{(K^+)} = 1.5 \times 10^{-3}$ (M/cm), the value of R_s for $L = 10$ (cm) is smaller than that for $L = 50$ (cm); this relationship will be inverted if $g_{(K^+)}$ increases further.

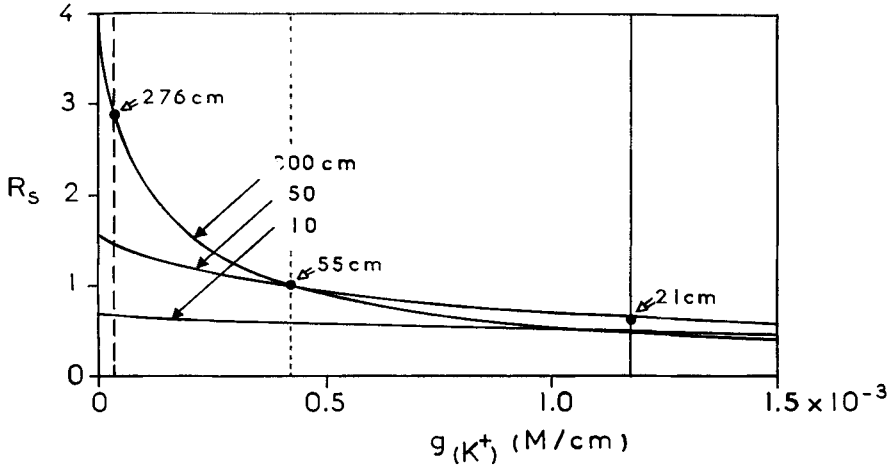

FIG. 4. Chromatographic resolution R_s for the mixture of lysozyme and a hypothetical molecule with the same dimensions as those of lysozyme ($x' = 7$) but with a slightly larger value of ln q (considered in Figs. 2 and 3) for columns with different lengths 10, 50, and 300 cm as functions of $g_{(K^+)}$. Both molecules are adsorbed onto P crystal sites. The three vertical lines indicate the three $g_{(K^+)}$s in both Figs. 1 and 2, and the three points indicated by arrows on the three vertical lines show the chromatographic resolutions obtained under experimental conditions identical with those for the three points indicated by arrows in Fig. 1. (For details, see text.)

and a column length of 300 cm. It can be seen in Fig. 4 that the maximum value of R_s is only about 1.4 times as large as the value 2.87 for the experimental point on the left-hand side, or the point indicated by the right-hand side arrow in Fig. 1. The experimental condition for this point, therefore, is close to the best possible condition that can be realized by using a column with a length less than 300 cm.

Figure 5 illustrates theoretical chromatograms as functions of $m_{(K^+)}$, calculated by Eqs. (A1) and (A2), for the mixture of lysozyme (left-hand-side pattern in each part of the figure) and the hypothetical molecule (right-hand-side pattern), under the three experimental conditions for the three points indicated by arrows in Fig. 1 or the three points in Fig. 4. The experimental conditions in Parts (a), (b), and (c) of Fig. 5 correspond to the conditions for the points in Fig. 1 indicated by the left-hand-side, the intermediate, and the right-hand-side arrows, or the conditions for the right-hand-side, the intermediate, and the left-hand-side points in Fig. 4, respectively. In Fig. 5 are also shown the centers of gravity, the lower and upper limits of the standard deviations of the chromatographic peaks (indicated on horizontal lines), and the elution molarities of the sharp

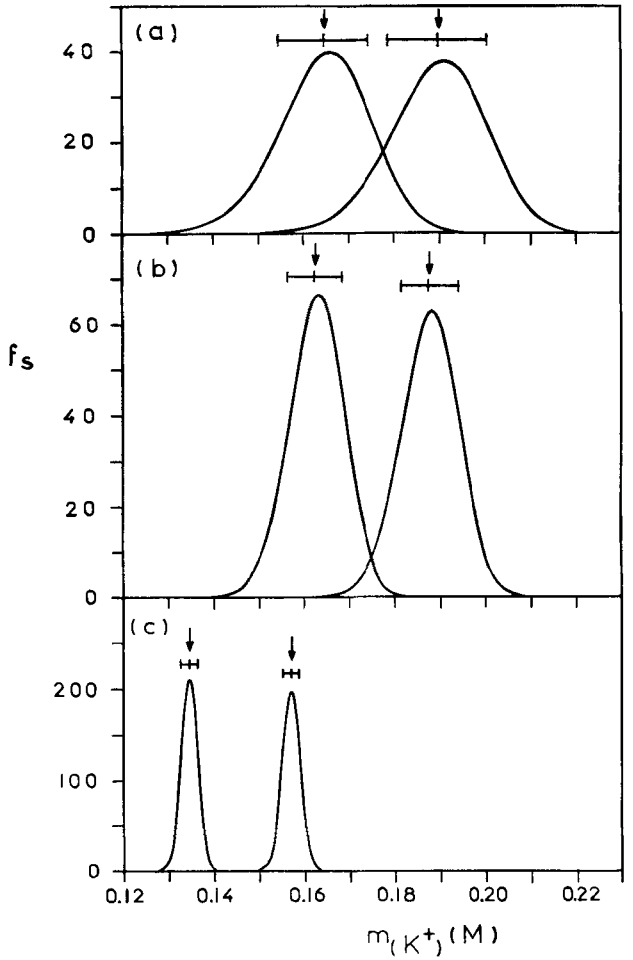

FIG. 5. Theoretical chromatograms, as functions of $m_{(K^+)}$, for the mixture of lysozyme (left-hand-side pattern in each part) and the hypothetical molecule considered in Fig. 4 (right-hand-side pattern) under three different experimental conditions, where $R_s = 0.60$, 1.01, and 2.87, respectively. The conditions in Parts (a), (b), and (c) are the same as those for the points in Fig. 1 indicated by the left-hand side, the intermediate, and the right-hand-side arrows, and the right-hand side, the intermediate, and the left-hand-side points in Fig. 4, also indicated by arrows, respectively. The centers of gravity and the lower and upper limits of the standard deviations of the chromatographic peaks (indicated on the horizontal lines), and the elution molarities of the sharp peaks obtained, provided there is no longitudinal molecular diffusion in the column (indicated by arrows), are also shown. The experimental chromatograms of lysozyme that correspond to the left-hand-side patterns in Parts (a), (b), and (c) are illustrated in Parts (a), (b), and (c) of Fig. 6, respectively. (For details, see text.)

peaks (obtained provided there is no longitudinal molecular diffusion in the column) calculated by Eq. (A14) (indicated by arrows). It can be seen in Fig. 5 that the shape of the chromatograms is almost Gaussian, and that the centers of gravity of the peaks almost coincide with the elution molarities of the sharp peaks, provided there is no longitudinal diffusion in the column. It can clearly be seen in Fig. 5 how the resolution of the column changes with a change in experimental conditions.

Parts (a), (b), and (c) of Fig. 6 illustrate three experimental chromatograms of lysozyme that correspond to the three points in Fig. 1 indicated by the left-hand-side, the intermediate, and the right-hand-side arrows. The left-hand-side patterns in Parts (a), (b), and (c) of Fig. 5, therefore, represent the theoretical chromatograms for the experimental patterns in the corresponding parts of Fig. 6. In Fig. 6 are also shown the centers of gravity and the lower and upper limits of the standard deviations of the peaks. In comparing Parts (a) and (b) of Fig. 6 with the corresponding parts of Fig. 5, it can be seen that the width of the experimental chromatograms is slightly smaller than that of the theoretical peaks. This is due to the fact that the experimental chromatograms with smaller than average values of the standard deviation, which are assumed to be theoretical values, have been chosen as examples (see Fig. 1). Slight differences in mean elution molarities between the experimental and theoretical peaks seen in Figs. 6 and 5 should also be due to the fluctuation in these values around the average values in the experimental chromatograms (cf. Figs. A1 and A2 in Appendix II). Further, it appears that the experimental chromatograms, in general, are slightly asymmetrical, with a slower decrease in height on the right-hand side of the pattern than on the other side (see Fig. 6). On the other hand, with the theoretical chromatograms it is on the left-hand side of the pattern that the height decreases more slowly, although the difference in rates of decrease in height between the two sides of the peak is extremely small and the peak is almost symmetrical (see Fig. 5). It can be suggested that this slight difference between the theoretical and experimental results might show a limit of the approximation of the introduction of Eq. (27) into Eq. (5) in Ref. *1*, respectively. In fact, Eq. (27) in Ref. *1*, which is valid with gradient chromatography, is derived from Eq. (21) in Ref. *1*, and introducing Eq. (21) in Ref. *1* into the general theory of chromatography corresponds to introducing a delta-function, Eq. (A42), into Eq. (A41) in Ref. *1*, Appendix III, as the initial condition. This also corresponds to introducing the delta-function, Eq. (A40), into Eq. (A39) in Ref. *1*, Appendix III, in the case of stepwise elution. The limit of the approximation of the delta-function was discussed in Ref. *1*, Appendix III. In two other papers (Refs. *7* and *8*, Appendix II), it was shown by using another approximation that, at least when

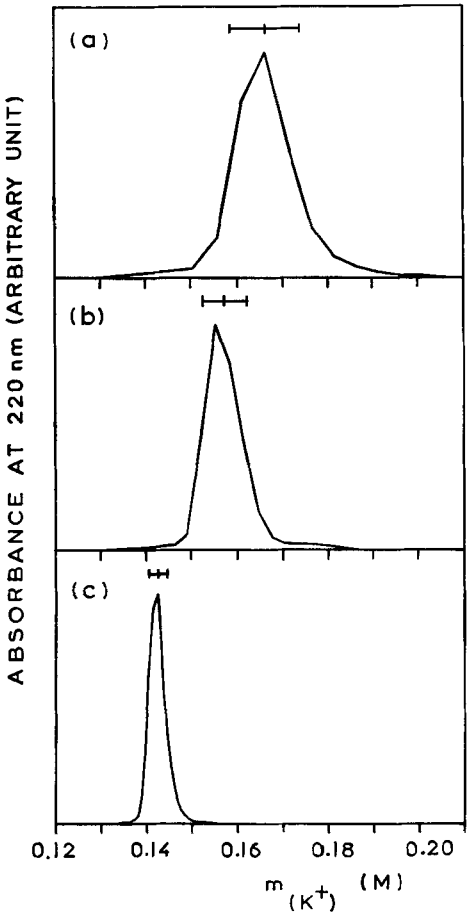

FIG. 6. Part (a), (b), and (c) illustrate three experimental chromatograms as functions of $m_{(K^+)}$, of lysozyme (at about 25 °C) that correspond to the points in Fig. 1 indicated by the left-hand-side, the intermediate, and the right-hand-side arrows, respectively. The corresponding theoretical chromatograms are shown in Parts (a), (b), and (c) of Fig. 5 (left-hand-side patterns). The centers of gravity and the lower and upper limits of the standard deviations of the peaks are also shown. (Reproduced, with modifications, from Fig. 8 of Ref. *2*.)

the column is extremely short or when the slope of the gradient of competing ions is almost zero, the chromatogram should have an asymmetrical shape that begins abruptly and finishes slowly with considerable tailing. [This is different from tailing or the deformation of the chromatogram occurring due to mutual energetical interactions among molecules adsorbed on the crystal surfaces of HA (cf. Ref. *8*).]

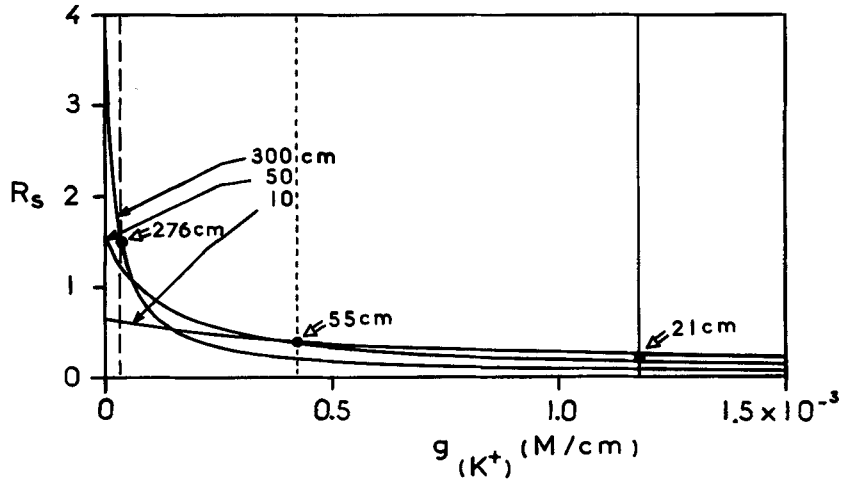

FIG. 7. As Fig. 4, but for the mixture of hypothetical molecules (adsorbed onto P sites) with the same value, 70, of x' (which is larger than the value, 7, for lysozyme) but with different values of ln q. This mixture was also considered in Fig. 2. (For details, see text.)

Figure 7 illustrates plots corresponding to those in Fig. 4 for a mixture of two hypothetical molecules with the same value, 70, of x'. This is 10 times as large as the value for lysozyme (see above). It is assumed that the values of ln q (Eq. A6) are 100.3 and 101.0 for respective components. Thus the difference between the two values of ln q, 0.7, is equal to the difference in the corresponding values between lysozyme and the hypothetical molecule considered above. It should be noted that the difference in ln q [$= x\varepsilon/kT + \ln(\beta\tau)$; see Eq. A6] between two molecules with the same dimensions or the same x' increases, in general, with an increase of x' if both ξ and τ are kept constant since $x = \xi x'$ (see Eq. A8). ξ, which represents the ratio of the total number, x, of the active functional groups per molecule to the dimensions, x', of the molecule, can be considered as a parameter with an intensive property that is related to the compositions and/or the sequences of amino residues in the case of protein. The value of ln q usually changes only slightly with a change of τ because τ is in the logarithmic term. Therefore, to increase x' of both components in the mixture while keeping the difference in ln q between the components constant corresponds to decreasing the difference in intensive properties between these molecules; it is the extensive difference that is kept constant. In Fig. 2, curves for molecules with $x' = 70$ (which are used for calculations of R_s) are also plotted where the curves of the respective components in the mixture cannot be distinguished. This is due to the small difference in

intensive properties between them. Now, by comparing Fig. 7 with Fig. 4, it can be found that, unless $g_{(K^+)}$ is extremely small, the resolution of the column generally decreases with an increase of x' if the difference of ln q between different molecules in the mixture is constant. However, when $g_{(K^+)}$ is small, and especially when L is large, R_s increases more rapidly with a decrease of $g_{(K^+)}$ when x' is large (Fig. 7) than when x' is small (Fig. 4). As a result, the limiting values of R_s to $g_{(K^+)} = +0$ M/cm when $x' = 70$ are almost equal to the values when $x' = 7$ for any column lengths (see Figs. 7 and 4). It can therefore be concluded that the larger the dimensions of any molecules in the mixture, the smaller is the minimum intensive structural difference between them that is necessary for the chromatographic separation under optimal experimental conditions.

It can also be seen in both Figs. 4 and 7 that R_s increases, in general, with a decrease of L if $g_{(K^+)}$ is large (cf. footnote on page 446), while it is when L is large that a large value of R_s is obtained if $g_{(K^+)}$ is small. To be precise, for any given finite value of $g_{(K^+)}$ there exists a finite value of L, denoted by L^*, that gives to R_s a maximum value, and it is L^* that increases with a decrease of $g_{(K^+)}$. L^* depends also on x'; for a given value of $g_{(K^+)}$, L^* decreases with an increase of x'. At the extremity, when $x' = \infty$, it is x', but not $g_{(K^+)}$, that determines the value of L^*. Thus, when $x' = \infty$, then $L^* = +0$ cm, independent of the value of $g_{(K^+)}$. On a column of infinitesimal length, R_s increases with a decrease of $g_{(K^+)}$, and the maximum value of R_s is obtained when $g_{(K^+)} = +0$ M/cm. (It should be noted, however, that these are the arguments provided the theory is valid even in extreme cases when L and $g_{(K^+)}$ tend to infinitesimal values.) Actually, it is impossible to carry out the chromatography with an infinitesimal value of $g_{(K^+)}$, and the optimal length of the column with a (virtually) minimum possible value of $g_{(K^+)}$ decreases with an increase of x'. In fact, when $g_{(K^+)} = 3.53 \times 10^{-5}$ M/cm (see the left-hand-side vertical lines in both Figs. 4 and 7), the R_s value for the column of length 300 cm is twice that for the column of length 50 cm if $x' = 7$ (Fig. 4). However, if $x' = 70$, the R_s values for the two column lengths are almost equal (Fig. 7).

In order to consider the optimal condition for the mixture of molecules with heterogeneous dimensions, it is necessary to take into account the fact that the dependences of $m_{elu(K^+)}$ on both L and $g_{(K^+)}$ are generally different with molecules with different dimensions. The larger the molecular dimensions x', the more slowly $m_{elu(K^+)}$ increases with increases of both L and $g_{(K^+)}$. When $x' = \infty$, $m_{elu(K^+)}$ is independent of both L and $g_{(K^+)}$. To have good resolution between large molecules with higher elution molarity and small molecules with lower elution molarity, $g_{(K^+)}$ should, in general, be small. This is because $\sigma_{(K^+)}$ for any chromatographic peak decreases with a decrease of $g_{(K^+)}$ (see Fig. 3), and $\Delta m_{elu(K^+)}$ increases with

a decrease of $g_{(K^+)}$ (or decreases more slowly than the decrease that occurs when any molecules have the same dimensions). If any molecules in the mixture have large enough dimensions, the best resolution of the column is attained, in general, when $g_{(K^+)}$ is small. In this instance, $\Delta m_{elu(K^+)}$ is independent of $g_{(K^+)}$ whereas $\sigma_{(K^+)}$ for any molecule decreases with a decrease of $g_{(K^+)}$ (see Fig. 3). As a general rule, the optimal column length decreases with an increase in the average dimensions of the molecules in the mixture. For the separation of large molecules with lower elution molarity and small molecules with higher elution molarity, it is impossible to find a general optimal condition unless the dimensions of these molecules are large enough (see above). This is because, under conditions where $\sigma_{(K^+)}$ decreases, $\Delta m_{elu(K^+)}$ decreases and vice versa. [In an earlier paper (*2*), the resolving power of the column was studied on the basis of several experiments, and essentially the same conclusions as those obtained in this paper were obtained. In the study in Ref. *2*, the resolution of the column was discussed in terms of the parameter α (rather than in terms of R_s) introduced in Ref. *2*, which is proportional to $1/\sigma$ in this paper. It can be considered that α in Ref. *2* represents, in fact, approximately the resolution of the column, since the change of R_s is governed mainly by the change of $\bar{\sigma}$ (see Eq. 1). This is the reason why essentially the same conclusions as those attained in this paper were obtained in Ref. *2*.]

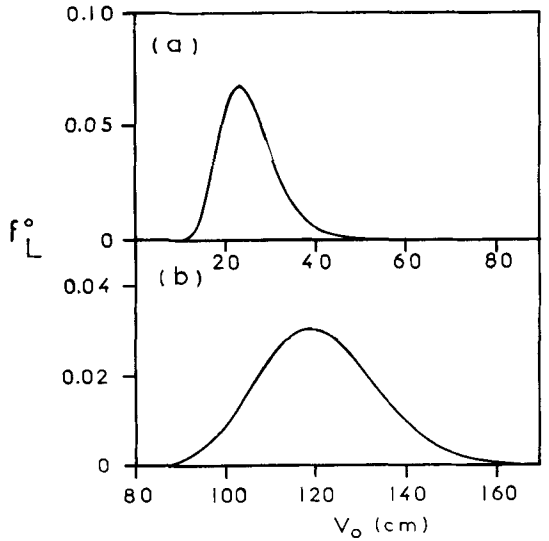

FIG. 8. Two theoretical chromatograms, with stepwise elution, for lysozyme obtained under different experimental conditions. (For details, see text.)

Finally, Fig. 8 illustrates two theoretical chromatograms with stepwise elution for lysozyme, calculated by Eq. (A16) and by using the value 0.3 cm for θ_0, for the case when $m_{(K^+)} = 0.165\ M$ [or when $m_{(P)} = 0.11\ M$; the subscript P indicates phosphate ions in the buffer] for two different column lengths, 10 cm (part a) and 50 cm (part b). Figure 8 can be compared with the experimental chromatogram for lysozyme in Fig. 6 in Ref. *9* obtained by Tiselius et al.

Collagen

Collagen is a structural protein with a molecular weight of about 3×10^5 daltons and is represented approximately by a rod of dimensions 3000×15 Å (*10*). It can be considered that collagen is adsorbed onto C crystal sites through carboxyl groups, and that the elution of the molecules is carried out by competition with phosphate ions from the buffer for C sites (*4*).

Parts (a), (b), and (c) of Fig. 9 illustrate three experimental chromatograms of calf-skin collagen [as functions of phosphate molarity, $m_{(P)}$, of the buffer] obtained under experimental conditions almost identical with those in Parts (a), (b), and (c) of Fig. 6, respectively. Thus the column lengths L are 21, 35, and 281 cm in Parts (a), (b), and (c) of Fig. 9, respectively (which can be compared with 21, 55, and 276 cm in the corresponding parts of Fig. 6). The slopes of the gradient of the phosphate buffer are identical between the corresponding parts of Figs. 9 and 6. It can therefore be estimated that the slopes of the gradient of competing phosphate ions [denoted by $g_{(P)}$] in Parts (a), (b), and (c) of Fig. 9 are 2/3 the $g_{(K^+)}$ in the corresponding parts of Fig. 6 (cf. the legend of Table 2), and are 7.85×10^{-4}, 2.83×10^{-4}, and $2.36 \times 10^{-5}\ M$/cm, respectively. It can clearly be seen in Fig. 9 that collagen is a heterogeneous protein and that the resolution of the column increases in the order of Parts (a), (b), and (c) with a multipeak chromatogram in Part (c). This can be compared with the chromatograms for lysozyme, a typical globular protein, illustrated in Fig. 6, where it can be seen that lysozyme is a highly homogeneous protein.

In order to analyze the experimental chromatograms in Fig. 9, it is necessary to know the value of φ' (see Eqs. A4 and A5) for competing phosphate ions. In Ref. *12* this value was estimated to be 6.7 or 4.6 M^{-1}. (In Ref. *12*, φ' was represented as a dimensionless quantity. φ' should have a dimension of M^{-1}, however.) It was also estimated (*12*) that if $\varphi' = 6.7\ M^{-1}$ and $\varphi' = 4.6\ M^{-1}$, the number of C sites on which the adsorption of phosphate ions is impossible due to the presence of the adenosine group of the ATP molecule (which is adsorbed on C sites by using the

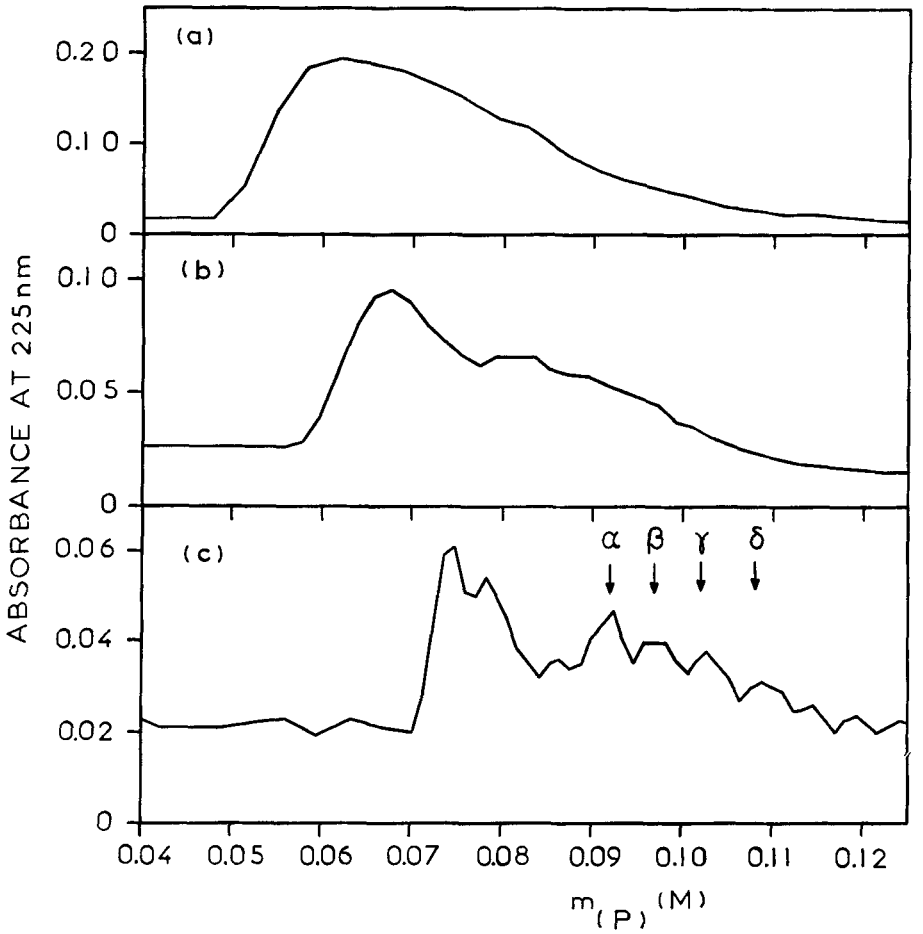

FIG. 9. Parts (a), (b), and (c) illustrate three experimental chromatograms, as functions of $m_{(P)}$, of calf-skin collagen (at 4°C) obtained under experimental conditions almost identical with those in Parts (a), (b), and (c) of Fig. 6, except that the sodium phosphate buffer at pH 6.8 (in contrast with the potassium buffer in experiments in Fig. 6) was used to make the gradient. Both 0.15 *M* NaCl and 1 *M* urea always exist in the buffer. Thus, in Parts (a), (b), and (c), the lengths *L* of the column are 21, 35, and 281 cm (in contrast with the lengths 21, 55, and 276 cm in the corresponding parts of Fig. 6), and the slopes, $g_{(P)}$, of the phosphate gradient are 7.85×10^{-4}, 2.83×10^{-4}, and 2.36×10^{-5} (*M*/cm) (which are identical with those in the corresponding parts of Fig. 6; for the relationship between $g_{(P)}$ and $g_{(K^+)}$, see the legend of Table 2), respectively. The presence of both sodium chloride and urea is necessary for collagen to be dissolved in the buffer. The concentration (1 *M*) of urea is far below that causing denaturation, which was verified on HA columns (*11*). [Parts (a), (b), and (c) are reproduced, with modifications, from Figs. 1, 2(B), and 6(E), respectively, of Ref. *11*.)

triphosphate chain) should be zero and unity, respectively. These two possibilities were examined by using a space-filling model of ATP. According to this study, on the surface of HA, ATP can take with comparable probabilities both the conformation in which the adenosine group of the molecule does not hinder the adsorption of the phosphate ion and the conformation in which it hinders the adsorption of only one phosphate ion. With a much smaller probability, ATP can take conformations in which the adenosine group covers more than one C site. It would be reasonable, however, to assume that ATP almost always takes the conformation in which the total number of C sites covered by the molecule is at a minimum, because the molecular structure of ATP seems to be flexible enough and, with this conformation, the (free) energy of the system seems to be minimized. Thus the calculation for the chromatography of collagen will be carried out mainly by using the value 6.7 M^{-1} of φ'.

The points in Fig. A3 in Appendix II are experimental plots of $\ln s_{(P)}$ versus the elution phosphate molarity, $m_{elu(P)}$, at which the maximum height of the collagen chromatogram is eluted when the sample load is small. The dotted straight line in Fig. 10 is the regression line for $m_{elu(P)}$ on $\ln s_{(P)}$ for these experimental points. Three continuous curves in Fig. 10 are theoretical, calculated from Eq. (A14) by using the value 6.7 M^{-1} of φ' and three different values of x'. The values of $\ln q$ were chosen for respective values of x' in order for the theoretical curves to coincide best with the regression line. It can be seen in Fig. A3 that a best fit between the theoretical curve and the regression line is obtained when $x' = 40$. The value 14.95 is obtained for $\ln q$ for the maximum height of the chromatogram. If it is assumed that $\varphi' = 4.6\ M^{-1}$, we have 50 and 13.54 for best values of x' and $\ln q$, respectively. (Figure A3 corresponds to Fig. A2 for lysozyme. The value 40–50 of x' obtained above is much smaller than the value estimated by assuming that no C sites existing under the adsorbed molecule can react with phosphate ions from the buffer. For this problem, see Ref. *13*.)

In the second and the third columns in Parts (a) and (b) of Table 1 are shown $m_{(P)}$ at the positions of the peaks α, β, γ, and δ indicated by arrows in Fig. 9(c), and the values of $\ln q$ for the corresponding peaks, calculated from Eq. (A14) and by using best values of 40 and 50 of x' for the possible values 6.7 and 4.6 M^{-1} of φ', respectively (see above). In parentheses in the third columns are shown the values of $\ln q$ obtained by assuming that the values of x' are smaller or larger, by a factor of 10, than the best values; these represent the limiting possible values (see Fig. A3 for the case when $\varphi' = 6.7\ M^{-1}$). In the fourth columns in Parts (a) and (b) of Table 1 are shown the differences, $\Delta \ln q$, of $\ln q$ between successive peaks in Fig. 9(c), calculated by assuming the best values and the two limiting values of

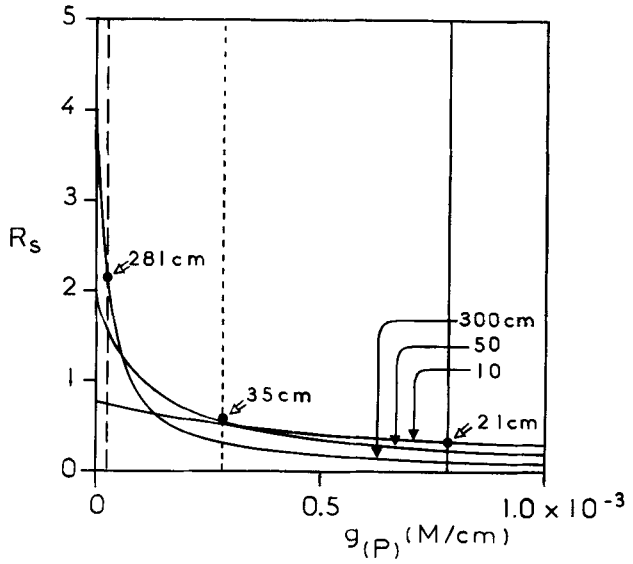

FIG. 10. Chromatographic resolutions R_s for the mixture of components β and γ of collagen [see Fig. 9(c)] with $x' = 40$ (adsorbed onto C sites) for columns with different lengths 10, 50, and 300 cm as functions of $g_{(P)}$. The three vertical lines indicate the three $g_{(P)}$s in Fig. 9, and the three points indicated by arrows on the three vertical lines show the chromatographic resolutions obtained under experimental conditions identical with those in parts (a), (b), and (c) of Fig. 9. This figure can be compared with both Figs. 4 and 7. (For details, see text.)

x' (see above). As the total number, about 230 (*14*), of carboxyl groups per molecule of collagen is large, it would be reasonable to assume that the ratio of the variation in values of τ (see Eq. A6) to the mean value is small among different collagen components, and that $\Delta \ln q$ essentially reflects the differences of $x\varepsilon/kT$ or x between molecules involved in successive peaks (see Eq. A6; for detailed consideration of τ for collagen, see Ref. *13*). It can be seen in Table 1 that the value of $\Delta \ln q$ is almost independent of the pair of successive peaks chosen for the calculation of this value. The same conclusion will be obtained if the peaks other than α, β, γ, and δ in Fig. 9(c) are chosen for the calculation of $\Delta \ln q$, since the intervals between any successive peaks are almost equal (see Fig. 9c). This would mean that the differences, $\Delta \ln q$, of $\ln q$ or $x\varepsilon/kT$ (see above) between any successive peaks are brought about by a common cause, which must be a stepwise variation in the number of carboxyl groups per molecule that react with adsorbing sites of HA. Thus the value of $kT\,\Delta \ln q$ must be almost equal to the value of ε, or the energy of adsorption onto a

TABLE 1

Differences in Energies of Adsorption per Molecule between Collagen Components Involved in Peaks α and β, Peaks β and γ, and Peaks γ and δ in the Chromatogram in Fig. 9(c)[a]

(a)

$\varphi' = 6.7\ (M^{-1})$, $x' = 40\ (30, 50)$				
Peak	$m_{(P)}$	$\ln q$	$\Delta \ln q\ (\approx \varepsilon/kT)$	ε (kcal/mol)
α	0.092	19.09(14.57, 23.67)	0.84(0.64, 1.05)	0.46(0.35, 0.58)
β	0.097	19.93(15.20, 24.72)	0.82(0.62, 1.03)	0.45(0.34, 0.56)
γ	0.102	20.76(15.83, 25.75)	0.97(0.73, 1.20)	0.53(0.40, 0.66)
δ	0.108	21.72(16.56, 26.95)		

(b)

$\varphi' = 4.6\ (M^{-1})$, $x' = 50\ (40, 60)$				
Peak	$m_{(P)}$	$\ln q$	$\Delta \ln q\ (\approx \varepsilon/kT)$	ε (kcal/mol)
α	0.092	17.56(14.25, 20.91)	0.82(0.66, 0.98)	0.45(0.36, 0.54)
β	0.097	18.38(14.90, 21.89)	0.80(0.65, 0.96)	0.44(0.36, 0.53)
γ	0.102	19.18(15.55, 22.85)	0.95(0.76, 1.14)	0.52(0.42, 0.63)
δ	0.108	20.13(16.31, 23.98)		

[a]Parts (a) and (b) represent the results obtained by using the values 6.7 and 4.6 M^{-1} for φ', respectively. In the outsides of the parentheses in the last three columns in both Parts (a) and (b) are shown the results obtained by using the best values 40 and 50 for x' for the respective values of φ' (see Fig. A3 in Appendix II for the case when $\varphi' = 6.7$ M^{-1}). In the parentheses in the last three columns are shown the results obtained by using the lower and upper limiting values of x' [which are 30 and 50 when $\varphi' = 6.7\ M^{-1}$ (see Fig. A3 in Appendix II), and 40 and 60 when $\varphi' = 4.6\ M^{-1}$, respectively]. For details, see text.

C site of a carboxyl group existing on the molecular surface of collagen. The values of ε obtained on the basis of this hypothesis are shown in the last column in Parts (a) and (b) of Table 1, the values in the outsides and the left- and right-hand sides in the insides of the parentheses being the values for the most probable and the lower and upper limiting possible values of x', respectively (see Fig. A3 for the case when $\varphi' = 6.7\ M^{-1}$). It should be recalled that, in Ref. *12*, the values 1.0 and 0.9 kcal/mol were obtained for the energy of adsorption onto a C site for a univalent phosphate group on the polyphosphate chain of nucleoside phosphates (by using the values 6.7 and 4.6 M^{-1} of φ', respectively). This is only about twice as large as the value, about 0.5 kcal/mol, of the energy for a carboxyl group estimated in Table 1. This would provide justification for the interpretation given above to the multipeak chromatogram of collagen.

In Refs. *15* and *16* a microheterogeneous model of collagen was pro-

posed. In Ref. *16*, almost the same value (0.5 kcal/mol) as those obtained in Table 1 was calculated for the adsorption energy of a carboxyl group of collagen by using an independent method based on the microheterogeneous model. This supports the microheterogeneous model itself.

It now is necessary to examine, by using the value 0.3 cm for the parameter θ_0 obtained on the basis of the experiment with lysozyme (see the section entitled "Lysozyme; Some Predictions Obtained from the Analysis"), whether or not we can explain the fact that the resolving power of the column under the experimental conditions in Parts (a), (b), and (c) of Fig. 9 increases in this order. It is also necessary to determine whether or not, under the condition in Part (c) of Fig. 9, the width of the theoretical peak for a single component of collagen is, in fact, comparable to, or slightly less than, the width of a peak in the experimental multipeak chromatogram in Fig. 9(c). It can be predicted that the width of each chromatographic peak broadens (slightly) due to repulsive interactions among molecules adsorbed on the crystal surface (*13*). It can be considered that if these points are, in fact, explained, the validity of the theory developed in Ref. *1* is confirmed even for the case when molecules are adsorbed onto C crystal sites. Several predictions made for molecules with different dimensions from those of lysozyme will also be verified, because collagen has much larger dimensions than those of lysozyme.

Figure 10 depicts plots corresponding to those in both Figs. 4 and 7 for components β and γ of collagen. In Fig. 10 are also shown the three slopes of the phosphate gradients (three vertical lines) and the resolutions of the column (three points) that are obtained under experimental conditions in Parts (a), (b), and (c) of Fig. 9, respectively. It can be seen in Fig. 10 that the limiting value of R_s to $g_{(P)} = +0\ M/\text{cm}$ when $L = 300$ cm (estimated by extrapolation) is about twice the value obtained when $g_{(P)} = 2.36 \times 10^{-5}\ M/\text{cm}$ and $L = 281$ cm (the left-hand-side point). This means that the value of R_s obtained under the experimental condition of Fig. 9(c) is only half the maximum possible value that can be realized when L is less than 300 cm (see Fig. 10).

Parts (a), (b), and (c) of Fig. 11 illustrate three theoretical chromatograms calculated by using Eqs. (A1) and (A2) for the mixture of components β and γ of collagen obtained under experimental conditions identical with those in Parts (a), (b), and (c) of Fig. 9, respectively. In Fig. 11 are also shown the centers of gravity and the lower and upper limits of the standard deviations of the peaks (shown on horizontal lines) calculated also by Eqs. (A1) and (A2), respectively. Elution molarities of the sharp chromatographic peaks that would be realized, provided there is no molecular diffusion in the column, have been calculated by Eq. (A14) and are also indicated by arrows. It can be seen in Fig. 11 that the resolving

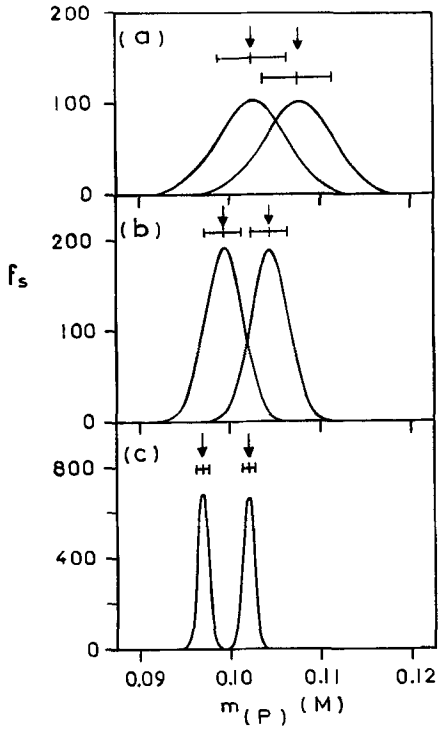

FIG. 11. Parts (a), (b), and (c) illustrate three theoretical chromatograms, as functions of $m_{(P)}$, for the mixture of components β and γ of collagen, where $R_s = 0.33$, 0.60, and 2.13, obtained under experimental conditions identical with those in Parts (a), (b), and (c) of Fig. 9 and those for the right-hand-side, the intermediate, and the left-hand-side points in Fig. 10, respectively. The centers of gravity and the lower and upper limits of the standard deviations of the chromatographic peaks (indicated on the horizontal lines), and the elution molarities of the sharp peaks obtained, provided there is no longitudinal molecular diffusion in the column (indicated by arrows), are also shown. This figure can be compared with Fig. 5. (For details, see text.)

power of the column under experimental conditions in Parts (a), (b), and (c) increases in this order, in parallel with its increase in the corresponding parts of Fig. 9, and that the widths of the peaks in Part (c) of Fig. 11 are slightly less than the widths of the peaks of components β and γ in Fig. 9(c). This confirms several predictions made in the lysozyme section (see above). It can be seen in Figs. 9 and 11, however, that the mean elution molarity of the experimental chromatogram increases whereas that for the two theoretical peaks decreases very slightly in Parts (a), (b), and (c) of the respective figures. This is perhaps due to experimental fortuity. [For a

measure of the range of fortuitous fluctuations in elution molarity, cf. Figs. A1–A3 in Appendix II, and Figs. 5(a) and (b) in Ref. *4*. In a subsequent paper (*13*), it will be shown that, with collagen, the repulsive interactions occurring on the crystal surfaces of HA importantly influence both the shape and the position of the chromatogram. By taking into account this effect and on the basis of the microheterogeneous model (see above), theoretical collagen chromatograms have been calculated under wider experimental conditions than those in Fig. 9; much better fits with the experiments have been obtained (*13*). The problem of mutual energetical interactions among molecules occurring on the crystal surfaces of HA is treated in a series of papers involving Refs. *8*, *15*, and *16*.]

Some Other Experiments

The theory was also examined by using cytochrome c; poly-L-lysine [adsorbed onto P sites (*4*, *5*)]; a mixture of ADP, ATP, and adenosine tetraphosphate [adsorbed onto C sites (*12*)]; and T_2 phage (see below). For cytochrome c, a satisfactory fit between theory and experiment was obtained. For the mixture of ADP etc., the widths of the experimental peaks were generally slightly smaller than those predicted by the theory. This can be presumed to be experimentally fortuitous. For poly-L-lysine the width of a peak in the experimental chromatogram shown in Fig. 1 in Ref. (*5*) was predicted theoretically. In this peak, several components with different τ values (see Eq. A6) should be involved (*5*); this was taken into consideration. A very good fit between theoretical and experimental results was obtained (*13*).

For T_2 phage we have no experimental data to show onto which site (P or C) it is adsorbed. However, when the particle has extremely large dimensions, the standard deviation σ_{V_0} of the chromatographic peak, expressed in terms of reduced elution volume V_0, should be independent of the slope of the molarity gradient of competing ions on whichever site the adsorption occurs, and σ_{V_0} should be represented by Eq. (A13). T_2 phage gives a single peak chromatogram on the HA column. Figure 1(E) in Ref. *2* shows that the elution phosphate molarity of the center of gravity of the T_2 phage peak is independent of both the length of the column and the slope of the gradient of the phosphate buffer. This demonstrates that the T_2 phage particle, which is known (*18*) to be constituted of a prolated icosahedral head of 650 × 950 Å and a tail of 250 × 1100 Å, in fact, has a very large value of x' which can be considered virtually infinite (cf. Eqs. A9, A10, and A15). Two types of points in Fig. 12 are experimental plots of σ_{V_0} for T_2 phage (when the sample load is extremely small) versus L for two different slopes of the gradient of phosphate buffer that are

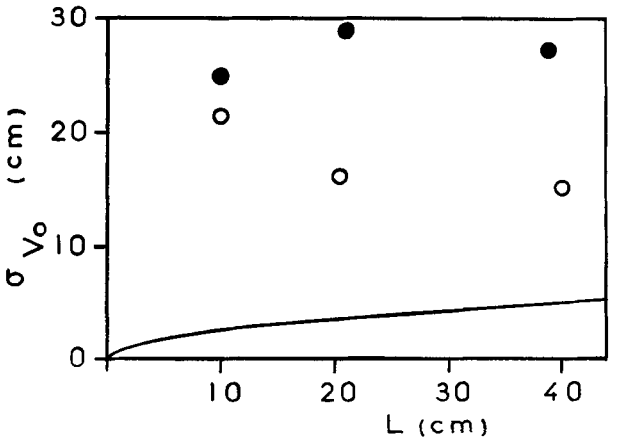

FIG. 12. Two types of points are experimental plots of σ_{V_0} of the chromatographic peaks of T_2 phage particles vs length L of the column for different slopes of the gradient of potassium phosphate buffer that are identical with those for the corresponding points in Fig. 1. (Reproduced, with modifications, from Fig. 9 in Ref. 2.) The curve is theoretical, calculated for any slope of the gradient of phosphate buffer by using the value 0.3 cm of θ_0, and by assuming that $x' = \infty$ and that the particles are completely homogeneous. The discrepancy between the experimental and theoretical results shows that T_2 particles should be heterogeneous. (For details, see text.)

identical with those for the same types of points in Fig. 1. The curve in Fig. 12 is theoretical, calculated from Eq. (A13) by using the value 0.3 cm of θ_0. Figure 12 shows that T_2 phage particles should be heterogeneous because, even taking into account the possible fluctuation in standard deviation of the experimental peaks (Fig. 1), the widths of the peaks of T_2 phage under any experimental conditions are evidently much larger than the widths which should be realized provided the particles are completely homogeneous (theoretical curve in Fig. 12). Also, σ_{V_0} should be independent of the slope of the gradient of competing ions provided the molecules are homogeneous (see above), whereas it can be seen in Fig. 12 that σ_{V_0} increases, in general, with a decrease in the slope of the gradient of the ions. This can be explained only by assuming that T_2 phage particles consist of different components with different characteristic elution molarities, and that the differences in elution volumes among different components increase with a decrease in the slope of the gradient of the ions, which extends σ_{V_0} of the total chromatogram. Here it should be added that an obviously heterogeneous chromatographic pattern of tobacco mosaic virus (TMV) was obtained by Mazin et al. (*19*) by using a column of granulated HA or a product consisting of spherical aggregate of the crystals synthesized in the presence of silica gel (*19*; cf. Table 2).

DISCUSSION

In the section entitled "Analysis of Several Experiments," it was shown theoretically that, at least for a mixture of molecules with the same dimensions, the larger the molecular dimensions, the smaller is the minimum intensive structural difference between molecules that is necessary for the chromatographic separation under optimal experimental conditions. It can be considered, however, that the high resolving power of the column for collagen obtained under an optimal condition (Fig. 9c) is due not only to the large dimensions of the molecules, but also to the fact that it is local structure on the molecular surface that determines the characteristic elution molarity of the rigid molecule, and not the total structure. This can be understood by recalling that the variation in the local intensive structure of a molecule among different components in a mixture should, in general, exceed the variation in the total molecular structure, and that the smaller the active local region on the molecular surface, the larger should be the variation. This is evident because the difference in total intensive structure between different molecules represents the difference in the average of the local structures within each molecule. In the case of lysozyme, it can be estimated (see Appendix IV in Ref. *5*) that it is only two or three functional basic groups out of the total of 18 (*3*) that can be used, at the same time, for the reaction with P sites. For collagen, it can be estimated (*13*) that it is only 15–25 carboxyl groups out of the total of 230 (*14*) that react at the same time with C sites. It should be noted, however, that the number of functional groups on the molecule that react at the same time with adsorbing sites of HA should, in general, be smaller than the total number of groups that effectively participate in the reaction with the adsorbing sites. This is because there should, in general, be more than one geometrical configuration of the molecule in which the same number of functional groups is adsorbed at the same time on the crystal sites, and the configuration should follow a Boltzmann distribution. Even taking into account these effects, it is likely that the number of functional groups on the molecular surface that effectively participate in the reaction with the crystal sites is, in general, much smaller than the total number of groups on the molecular surface. The situation is different in the case of DNA with a regular homogeneous distribution of functional phosphate groups on the molecular surface in the native state.

It can be concluded (see the sections entitled "Lysozyme; Some Predictions Obtained from the Analysis" and "Collagen") that, except in some special cases, it is always when the slope of the gradient of competing ions is extremely small that high resolutions of the column can be obtained. It would now be interesting to look upon the experimental conditions applied in some typical published works where chromatographic separations

TABLE 2

Some Typical Examples of the Experimental Conditions Applied to Linear Gradient Chromatographies on HA Columns in Published Works[a]

Mixture	Cation in phosphate buffer	Column height L (cm)	$g'_{(P)}$ (M/mL)	Authors	Refs.
Native and denatured calf thymus DNA[b]	Na^+	7	2.7×10^{-3}	Bernardi	Fig. 3C in Ref. *20*
Bacteriophage T_2 DNA and *Escherichia coli* DNA (native states)[c]	Na^+	3	5.5×10^{-3}	Oishi	Fig. 1 in Ref. *22*
Yeast (*Saccharomyces cerevisiae*) mitochondrial DNA's with different base compositions and dimensions, obtained by degradation with spleen DNase (native states)	Na^+	65	5.6×10^{-4}	Piperno, Fonty, and Bernardi	Figs. 1, 7, and 8 in Ref. *23*
Nuclear and mitochondrial native DNA's, and ribooligo nucleotides with different base compositions and dimensions, respectively, from yeast (*Saccharomyces cerevisiae*)	Na^+	40	1.8×10^{-3}	Piperno and Bernardi	Fig. 1 in Ref. *24*
Different types of *Escherichia coli* t-RNA	Na^+	68	2.0×10^{-4}	Pearson and Kelmers	Fig. 1 in Ref. *25*
Vulgare TMV-RNA's hydrolyzed with T_1 RNase[d]	Na^+	45	4.8×10^{-4}	Mundry	Fig. 3 in Ref. *26*
AMP, ADP, ATP, and adenosine tetraphosphate[e]	K^+	10	2.5×10^{-3}	Bernardi	Fig. 1 in Ref. *27*
Low molecular weight poly-L-lysine with different chain lengths[f]	Na^+	22	2.2×10^{-3}	Bernardi	Fig. 5(a) in Ref. *28*
Rabbit α and β hemoglobin chains (complexed with sodium dodecyl sulfate (SDS))[g]	Na^+	20	1.2×10^{-3}	Moss and Rosenblum	Fig. 1 in Ref. *29*
Different types of Vaccinia virus polypeptides (complexed with SDS)[g]	Na^+	20	1.2×10^{-3}	Moss and Rosenblum	Fig. 3 in Ref. *29*

B. Stearothermophilus enzymes containing: triose phosphate isomerase, glyceraldehyde 3-phosphate dehydrogenase, NADH dehydrogenase, and valyl-, methionyl-, and tryptophanyl-*t*-RNA synthetases[h]	K^+	18	4.4×10^{-3}	Atkinson, Bradford, and Selmes	Fig. 2 in Ref. *30*
TMV (which is heterogeneous)[i]	Na^+	18	6.1×10^{-4}	Mazin, Sulimova, and Vanyushin	Fig. 4(c) in Ref. *19*

[a]Unless stated, the phosphate buffer used for making the linear molarity gradient of ions is the equimolar mixture of NaH_2PO_4 and Na_2HPO_4, or KH_2PO_4 and K_2HPO_4, pH $\approx$ 6.8. The type of cation involved in the buffer is shown in the second column. As we do not always know on which of the C and P sites of HA the adsorption of the molecule occurs, and by which phosphate ions or cations from the buffer the desorption of the molecule is carried out, we always represent the slope of the gradient in terms of the phosphate ions in the buffer. The reduced value (to the column diameter 1 cm) of the parameter $g'_{(P)}$ is used, $g'_{(P)}$ representing the slope of the gradient expressed as the increase in phosphate molarity per unit elution volume [the fourth column, where the reduced value of $g'_{(P)}$ is written simply as $g'_{(P)}$]. The reduced $g'_{(P)}$ was written as grad in the earlier papers (*2, 12*) (see Fig. A1 in Appendix II). The reduced values of $g'_{(P)}$ in Parts (a), (b), and (c) of both Fig. 6 (where $g_{(K^+)} = 1.18 \times 10^{-3}$, 4.24×10^{-4}, and 3.53×10^{-5} *M*/cm) and Fig. 9 (where $g_{(P)} = 7.85 \times 10^{-4}$, 2.83×10^{-4}, and 2.63×10^{-5} *M*/cm) are 1.25×10^{-3}, 4.5×10^{-4}, and 3.75×10^{-5} *M*/mL, respectively. [We have relationships among $g_{(K^+)}$, $g_{(P)}$, and reduced $g'_{(P)}$ such that $g_{(P)} = 0.628 g'_{(P)}$ and that $g_{(K^+)} = 1.5 g_{(P)}$; cf. note for Table 2 in Ref. *12* and note for Table 1 in Ref. *5*]. It can be seen that, in published works, the reduced values of $g'_{(P)}$ are comparable with the value in Part (a) or (b) of both Figs. 6 and 9, and are much steeper than the value applied in Part (c) of these figures.

[b]The experimental condition in Fig. 3C in Ref. *20* is given in the legend for Fig. 9 in Ref. (*21*).

[c]The phosphate buffer at pH 7.0 is used for the elution of molecules.

[d]In the presence of 7 *M* urea.

[e]Figure 1 in Ref. *27* is reproduced, with slight modifications, as Fig. 3 in an earlier paper (*12*).

[f]Figure 5(a) in Ref. *28* is reproduced, with slight modifications, as Fig. 1 in an earlier paper (*5*).

[g]The phosphate buffer at pH 6.4, containing 0.1% SDS and 1 m*M* dithiothreitol, is used for the elution of molecules.

[h]In the presence of 10 m*M* β-mercaptoethanol.

[i]The chromatography is carried out by using granulated HA or the product consisting of spherical aggregates of the crystals, synthesized in the presence of silica gel particles, and an obviously heterogeneous chromatographic pattern is obtained (cf. the section entitled "Some Other Experiments"). In the legend for Fig. 4(c) in Ref. *19*, the information for the shape of the column is not stated. However, this is presumably 18 $\times$ 0.7 cm, by referring to the section entitled "Material and Methods" in Ref. *19*.

of several types of molecular mixtures were performed on HA columns. These are summarized in Table 2. It can be seen in Table 2 that, in any instance, the slope of the gradient of competing ions that was applied is comparable with that used in Part (a) or (b) of both Figs. 6 and 9, and much steeper than that used in Part (c) of these figures (see the footnotes of Table 2). It can, therefore, be expected that much higher chromatographic resolutions would generally be obtained in these experiments if much smaller slopes of the gradient and the columns with optimal lengths are applied.

It is of interest that, in the experiment involving Vaccinia virus structural polypeptides in Table 2, it was found that a considerable chromatographic separation of some of these polypeptides with virtually the same electrophoretical mobility (on polyacrylamide gel) occurs on the HA column, even under the experimental condition where the slope of the gradient of phosphate buffer that is applied is almost equal to that in Part (a) of both Figs. 6 and 9 (*29*). This can be compared with the case of collagen when two types of polypeptide chains (α_1 and α_2 chains) that combine to form the whole collagen molecule by constituting a triple helix (with two α_1 and one α_2 chain) (*10*, *31*) give, respectively, single bands in electrophoreses on both acrylamide and starch gels as well as in chromatography on CM-cellulose columns (*31*). Nevertheless, the whole collagen molecule (with a rigid tertiary structure) gives multipeak chromatograms on HA columns (under optimal experimental conditions; see Fig. 9c). [The possibility that both α_1 and α_2 chains (with a constant ratio of 2:1, in number) are distributed at random among different collagen molecules, producing four types of molecules, $(\alpha_1, \alpha_1, \alpha_1)$, $(\alpha_1, \alpha_1, \alpha_2)$, $(\alpha_1, \alpha_2, \alpha_2)$ and $(\alpha_2, \alpha_2, \alpha_2)$, can almost be excluded. It can be considered that each molecule can be represented by $(\alpha_1, \alpha_1, \alpha_2)$ (see Refs. *10* and *31*).]

APPENDIX I

The equations that represent theoretical chromatograms for each component in a mixture for some different cases involving small sample loads (*1*) are summarized below, including the explanations of the physical meanings of any symbols.

Equations (36′) and (34) in Ref. *1* (hereafter, the number of the equation which does not bear the index "A" indicates the number in Ref. *1*), viz.,

$$f_s(m) = \frac{1}{\sqrt{4\pi\theta_0 gs}} \cdot e^{-(r(m_\lambda)-s)^2/4\theta_0 gs} \frac{\dfrac{dr(m_\lambda)}{dm_\lambda}}{1 + \dfrac{dr(m_\lambda)}{dm_\lambda}} \tag{A1}$$

and

$$m = m_\lambda + r(m_\lambda) - s \tag{A2}$$

represent a chromatogram developed by linear gradient elutions. This is performed under a given experimental condition characterized by a parameter s (see below) as a function of molarity, m, of competing ions, using m_λ (a parameter with a dimension of molarity) as an intermediate parameter. In Eqs. (A1) and (A2), θ_0 (with a dimension of length) is a positive constant that measures the longitudinal diffusion of molecules in the column (see Eqs. 21 and 37, and Eq. A37 in Ref. *1*, Appendix III). s (with a dimension of molarity) is defined (Eq. 25) as

$$s = gL \tag{A3}$$

where (and in Eq. A1) g is a positive constant that represents the slope of the molarity gradient of competing ions on the column, expressed as the increase in molarity per unit length of the column (measured from the bottom to the top). L represents the length of the column. Therefore, under any given experimental condition, or when the values of both L and g are fixed, s has a constant value. $r(m_\lambda)$ and $dr(m_\lambda)/dm_\lambda$ are defined by Eqs. (11) and (12) as

$$r(m_\lambda) = \frac{1}{q\varphi'(x' + 1)}[(\varphi' m_\lambda + 1)^{x'+1} - (\varphi' m_{\text{in}} + 1)^{x'+1}] \tag{A4}$$

and

$$\frac{dr(m_\lambda)}{dm_\lambda} = \frac{1}{q}(\varphi' m_\lambda + 1)^{x'} \tag{A5}$$

where m_{in} is the initial molarity of competing ions at the beginning of the gradient and x' is the average number (in the equilibrium state) of adsorbing sites of HA on which the adsorption of competing ions is impossible due to the presence of an adsorbed sample molecule. x' represents, therefore, the effective dimensions of the molecule. φ' represents the ratio, to molarity m or m_λ, of the "force" endowed with competing ions which drives the sample molecules out of the crystal surface; the ions drive the sample molecules through competition mechanism. Therefore, the "driving force" itself can be represented by $\varphi' m$ or $\varphi' m_\lambda$. It can be assumed that φ' is essentially (positively) constant throughout the chromatographic process. This means that the "driving force" of the ions is virtually proportional to molarity m or m_λ. In Eqs. (A4) and (A5), q is defined by Eq. (A2) in Appendix I of Ref. *1* or as

$$q = \beta\tau e^{x\varepsilon/kT} \tag{A6}$$

where x is the average number (in the equilibrium state) of functional groups per molecule that react with sites of HA, $-\varepsilon$ ($\varepsilon > 0$) is the adsorption energy of a functional group of the molecule on to one of the sites of HA, T is the absolute temperature, k is the Boltzmann constant, and β and τ are positive constants related, respectively, to the properties of the column and those of the molecule. Thus, neglecting a solvent effect, τ represents the number of effective geometrical configuration(s) of a sample molecule on the crystal surface (in equilibrium state), and is related, in general, to both distribution of functional groups on the molecular surface and the flexibility (or the rigidity) of the molecular structure. In the special case where the flexibility (or the rigidity) of the molecular structure is the same in both solution and the adsorbed state, which should be true with rigid or native molecules, τ should be related only to the distribution of the adsorption groups on the molecular surface. Therefore, if ε is large, τ should represent the number of energetically most stable geometrical configuration(s) of the molecule on the crystal surface. $f_s(m)$ is normalized such that

$$\int_{m_{in}}^{\infty} f_s(m)\, dm = 1 \tag{A7}$$

When $x' = \infty$ and when

$$\xi = x/x' \tag{A8}$$

has a finite value, i.e., in the case of molecules with very large dimensions, Eqs. (A1) and (A2) reduce to a single equation, Eq. (45), or to

$$f_s(m) = \frac{1}{\sqrt{4\pi\theta_0 gs}} e^{-(m-m^\circ)^2/4\theta_0 gs} \tag{A9}$$

where m° is defined by Eq. (42) as

$$m^\circ = \frac{1}{\varphi'}(e^{\xi\varepsilon/kT + (\ln \tau)/x'} - 1) \approx \frac{1}{\varphi'}(e^{\xi\varepsilon/kT} - 1) \tag{A10}$$

It should be noted that Eq. (A9) represents a Gaussian distribution with both the maximum height and the center of gravity always at $m = m^\circ$ (i.e., independently of both length, L, of the column and slope, g, of the gradient of competing ions), and with the standard deviation (with a dimension of molarity)

$$\sigma = \sqrt{2\theta_0 gs} \tag{A11}$$

which can be rewritten, with Eq. (A3), as

$$\sigma = \sqrt{2\theta_0 Lg} \tag{A11'}$$

The standard deviation can also be expressed in unit of reduced elution volume V_0 (with a dimension of length), which is defined by Eq. (48) or as

$$V_0 = V/\alpha \tag{A12}$$

where V is the actual elution volume and α (with dimensions of area) represents the pore volume per unit length of the column. Thus, dividing Eq. (A11′) by g,

$$\sigma_{V_0} = \sqrt{2\theta_0 L} \tag{A13}$$

is obtained. It can be seen in Eq. (A13) that σ_{V_0} is independent of the slope of the molarity gradient of competing ions, and that it increases simply with an increase of L.

The shape of the chromatographic peak is generally almost symmetrical (in the case of gradient elution), and the molarity of competing ions at which the maximum height occurs and the molarity at which the center of gravity of the peak is eluted can be represented approximately by Eq. (40′). This equation describes the dependence of the elution molarity, m, of the sharp peak of the sample molecules upon s, provided there is no longitudinal molecular diffusion in the column. This equation can be written as

$$m = \frac{1}{\varphi'}\{[(x' + 1)\varphi' qs + (\varphi' m_{\text{in}} + 1)^{x'+1}]^{1/(x'+1)} - 1\} \tag{A14}$$

When $x' = \infty$ and when ξ has a finite value (see above), Eq. (A14) reduces to

$$m = m^{\circ} \tag{A15}$$

Finally, Eq. (A35′) in Ref. *1* Appendix III, viz.,

$$f^{\circ}{}_L(V_0) = \sqrt{\frac{B}{4\pi\theta_0 V_0}}\, e^{-(L - BV_0)^2/4\theta_0 BV_0} \tag{A16}$$

represents the chromatogram, using stepwise elution, for a column of length L as a function of reduced elution volume V_0 and B represents the partition of a given component of a mixture in the interstitial liquid within a given section of the column, or the ratio of the amount of any given molecules in solution to the total amount of these molecules in that column section. In stepwise elution, B is constant throughout the chromatographic process. $f^{\circ}{}_L(V_0)$ is normalized such that

$$\int_0^{\infty} f^{\circ}{}_L(V_0)\, dV_0 = 1 \tag{A17}$$

APPENDIX II

Figures related to the experimental analysis made by using Eq. (A14) in Appendix I are summarized below. Equation (A14) is the equation that was first derived several years ago on the basis of a primitive consideration on the chromatographic mechanism (Eq. 15 in Ref. *4*). Theoretical curves in Fig. A2 and one of the curves in Fig. A3 had been published (with experimental data) before Ref. *1* was written. However, Eq. (A14) now is part of the theory developed in Ref. *1*, and the figures below are useful for the verification of this theory.

Figure A1. Experimental plots of elution molarities at the centers of gravity of lysozyme chromatographic peaks versus length, L, of the column for three different slopes of the molarity gradient. Elution molarity is expressed as molarity concerning phosphate ions in the buffer. This is 2/3 the molarity of competing potassium ions (see the legend of Table 2). The experimental values of the three slopes of the gradient are given, instead of in $g_{(K^+)}$, in terms of the reduced $g'_{(P)}$ to the column diameter 1 cm (written as grad). The relationship among the three different expressions of the slope of the gradient [viz., $g_{(K^+)}$, $g_{(P)}$, and reduced $g'_{(P)}$ (= grad)] are given in the footnotes of Table 2. Experimental values of grad in the three series of chromatographies 1.2–1.5 × 10^{-3}, 4.2–5.1 × 10^{-4}, and 3.6–

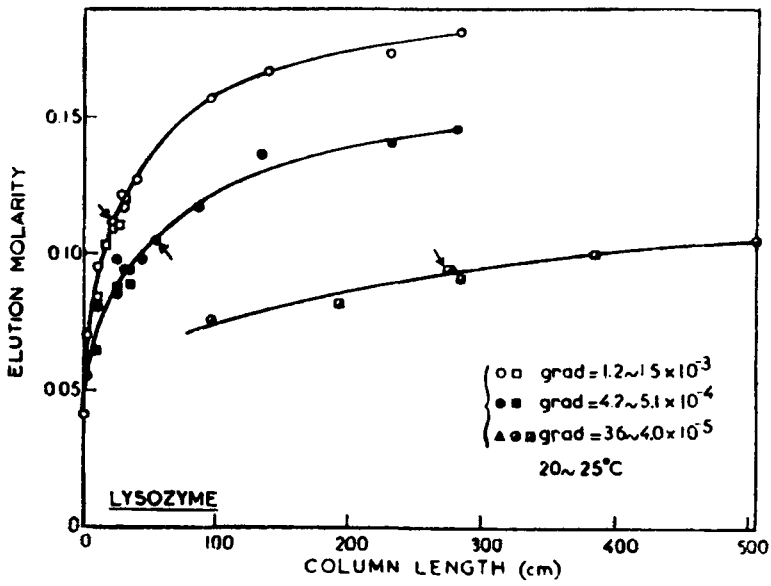

FIGURE A1.

4.0×10^{-5} M/mL coincide, within the limit of the experimental errors, with the theoretical values 1.25×10^{-3}, 4.5×10^{-4}, and 3.75×10^{-5} M/mL, respectively (cf. Ref. *8*). The corresponding $g_{(K^+)}$ values can be estimated to be 1.18×10^{-3}, 4.24×10^{-4}, and 3.53×10^{-5} M/cm, respectively (see the footnotes of Table 2). Three points indicated by arrows correspond to the three points also indicated by arrows in both Figs. A2 and 1 (reproduced, with slight modifications, from Fig. 2A in Ref. *2*).

Figure A2. Points: plots of experimental points in Fig. A1 on a ($m_{elu(K^+)}$, ln $s_{(K^+)}$) plane. Three points indicated by small arrows correspond to the three points also indicated by arrows in both Figs. A1 and 1. It can be seen that all the experimental points in Fig. A1 converge into a single array on the ($m_{elu(K^+)}$, ln $s_{(K^+)}$) plane. The continuous curves are theoretical, calculated by using Eq. (A14). A best fit with the experiment can be obtained assuming $x' = 7$, $\varphi' = 9\ M^{-1}$, and ln $q = 6.7$; these are reasonable values. [Reproduced with slight modifications from Fig. A7(b) in Ref. *5*, Appendix IV; an unfilled circle in that figure has been corrected to a filled circle. For theoretical curves with $x' \leqslant 6$, see Fig. A7(a) in Ref. *5*, Appendix IV.]

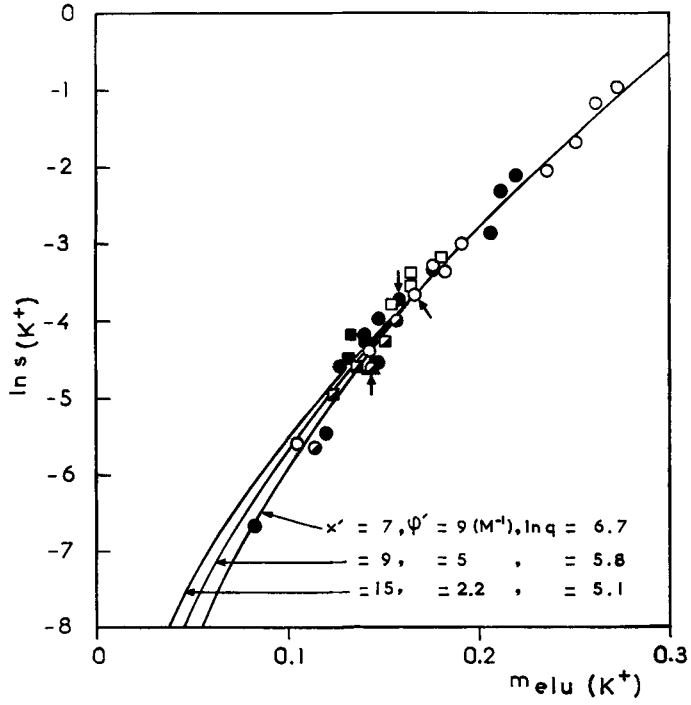

FIGURE A2.

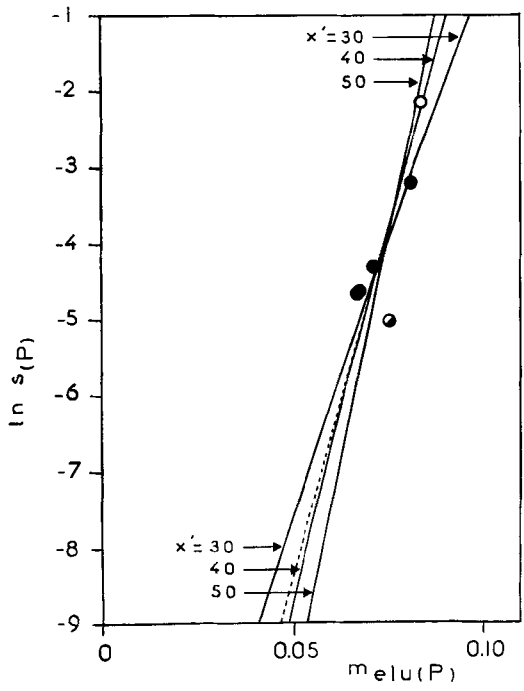

FIGURE A3.

Figure A3. The points are experimental plots of $\ln s_{(P)}$ versus elution phosphate molarity, $m_{elu(P)}$, at which the maximum height of the collagen chromatogram is eluted when the sample load is small. The dotted straight line is the regression line for $m_{elu(P)}$ on $\ln s_{(P)}$ for these experimental points. [Reproduced from Fig. 5(c) in Ref. *4*, respectively]. The point ◕ corresponds to the chromatogram in Fig. 9(c). Three continuous curves (which are almost straight lines) are theoretical, calculated from Eq. (A14) by using the value 6.7 M^{-1} of φ' and three different values of x'. The values of $\ln q$ were chosen for respective values of x' in order for the theoretical curves to coincide best with the regression line. It can be seen that a best fit between the theoretical curve and the regression line can be obtained when $x' = 40$. (For details, see text.)

Acknowledgments

The author is grateful to Dr. G. Bernardi for useful discussions and interest in this work, and thanks the Centre National de la Recherche Scientifique, Paris, for financial support. He also wishes to thank Dr. A.

Hudson for his kind editorial help. Calculations were performed on the CDC 6600 computer of the Faculty of Sciences, University of Paris.

REFERENCES

1. T. Kawasaki, *Sep. Sci. Technol.*, *16*, 325 (1981).
2. T. Kawasaki and G. Bernardi, *Biopolymers*, *9*, 257 (1970).
3. T. Imoto, L. N. Johnson, A. C. T. North, D. C. Phillips, and J. A. Pulpley, in *The Enzymes*, Vol. 7 (P. D. Boyer, ed.), Academic, New York, 1972, p. 665.
4. T. Kawasaki, *J. Chromatogr.*, *93*, 313 (1974).
5. T. Kawasaki, *Ibid.*, *157*, 7 (1978).
6. J. C. Giddings, *Dynamics of Chromatography: Part I, Principles and Theory*, Dekker, New York, 1965, p. 13.
7. T. Kawasaki, *J. Chromatogr.*, *120*, 271 (1976).
8. T. Kawasaki, *Ibid.*, *161*, 15 (1978).
9. A. Tiselius, S. Hertén, and Ö. Levin, *Arch. Biochem. Biophys.*, *65*, 312 (1956).
10. W. Traub and K. A. Piez, *Adv. Protein Chem.*, *25*, 243 (1971)
11. T. Kawasaki and G. Bernardi, *Biopolymers*, *9*, 269 (1970).
12. T. Kawasaki, *J. Chromatogr.*, *151*, 95 (1978).
13. T. Kawasaki, Submitted for Publication.
14. J. E. Eastoe, in *Treatise on Collagen*, Vol. 1 (G. N. Ramachandran, ed.), Academic, New York, 1967, p. 1.
15. T. Kawasaki, *J. Chromatogr.*, *82*, 219 (1973).
16. T. Kawasaki, *Ibid.*, *82*, 237 (1973).
17. T. Kawasaki, *Ibid.*, *93*, 337 (1974).
18. S. E. Luria and J. E. Darnell, Jr., *General Virology*, 2nd ed., Wiley, New York, 1967, p. 187.
19. A. L. Mazin, G. E. Sulimova, and B. F. Vanyushin, *Anal. Biochem.*, *61*, 62 (1974).
20. G. Bernardi, *Nature (London)*, *206*, 779 (1965).
21. G. Bernardi, *Methods Enzymol.*, *21*, 95 (1971).
22. M. Oishi, *Ibid.*, *21*, 140 (1971).
23. G. Piperno, G. Fonty, and G. Bernardi, *J. Mol. Biol.*, *65*, 191 (1972).
24. G. Piperno and G. Bernardi, *Bull. Soc. Chim. Biol.*, *52*, 885 (1970).
25. R. L. Pearson and A. D. Kelmers, *J. Biol. Chem.*, *241*, 767 (1966).
26. K. W. Mundry, *Z. Vererbungslehre*, *97*, 281 (1965).
27. G. Bernardi, *Biochim. Biophys. Acta*, *91*, 686 (1964).
28. G. Bernardi, *Methods Enzymol.*, *22*, 325 (1971).
29. B. Moss and E. N. Rosenblum, *J. Biol. Chem.*, *247*, 5194 (1972).
30. A. Atkinson, P. A. Bradford, and I. P. Selmes, *J. Appl. Chem. Biotechnol.*, *23*, 517 (1973).
31. K. A. Piez, in *Treatise on Collagen*, Vol. 1 (G. N. Ramachandran, ed.), Academic, New York, 1967, p. 207.

Received by editor September 26, 1980